

Constraints on a synthetic-noise source for Johnson noise thermometry*

D R White¹ and S P Benz

National Institute of Standards and Technology, 325 Broadway, Boulder, CO 80305-3328, USA

Received 12 October 2007

Published 18 January 2008

Online at stacks.iop.org/Met/45/93

Abstract

Conventional Johnson noise thermometers based on switching correlators have conflicting matching requirements for the sensing resistance. To mitigate distortion effects in the correlator, the RT products of the two sensors must be the same, and to mitigate frequency-response errors in nominally identical input circuits, the two sensing resistances should be the same. A noise thermometer using synthetic noise for the primary reference signal overcomes this conflict because the output voltage and output resistance are independent. This paper presents the rationale and design constraints for a noise thermometer using a synthetic-noise source based on Josephson junctions. The quantized voltage noise source developed at NIST produces tunable waveforms with a spectral density composed of a comb of frequencies of equal amplitude and random phase. In addition to the conventional noise-power and impedance constraints, it has additional constraints relating to the number of tones and the tone spacing.

(Some figures in this article are in colour only in the electronic version)

1. Introduction

In Johnson noise thermometry, temperature is inferred from a measurement of the thermal voltage generated across a resistor. According to Nyquist's law, the mean-square voltage is

$$\overline{V_T^2} = 4kT R \Delta f, \quad (1)$$

where T is the temperature, k is Boltzmann's constant, R is the resistance of the sensing resistor and Δf is the bandwidth over which the noise is measured. Currently the most accurate noise thermometers are based on the switching-correlator design first proposed by Brixy [1, 2], shown in simplified schematic form in figure 1.

The correlator is used to ensure that the measurement of the noise power (1) is independent of the input noise voltage of the preamplifier [3, 4], while frequent switching between the two sensing resistances, at different temperatures, eliminates the effects of drifts in the noise thermometer gain and frequency response. If the bandwidths and gains of the noise thermometer are the same for both measurements of noise

* This work is a contribution of an agency of the US Government and is thus not subject to US copyright.

¹ Currently a Guest Researcher at NIST. Permanent address: Measurement Standards Laboratory, PO Box 31310, Lower Hutt 5040, New Zealand.

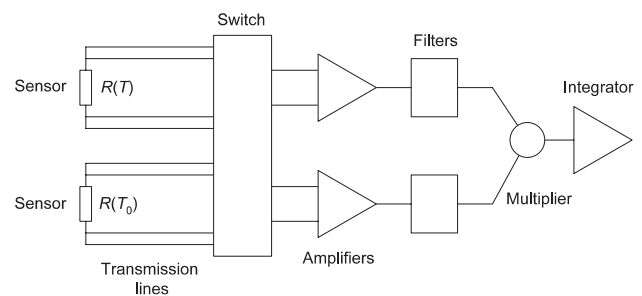


Figure 1. Simplified schematic diagram of a conventional switching-correlator noise thermometer.

power, an unknown temperature can be inferred from the ratios of the measured noise powers and the sensing resistances:

$$T = T_0 \frac{\overline{V_T^2} R(T_0)}{\overline{V_{T_0}^2} R(T)}, \quad (2)$$

where T is the unknown temperature and T_0 is the reference temperature (often the triple point of water).

Most noise thermometers employing the switching-correlator design use digital electronics for the multiplying and integrating stages of the thermometer. Digital processing has the advantages of enabling compact storage of random

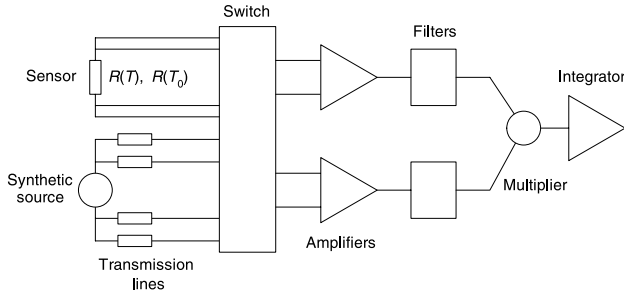


Figure 2. A simplified schematic diagram of the new noise thermometer using a synthetic reference.

data as averaged cross-spectra, eliminating the effects of the analogue filter response, enabling digital definitions of the correlation bandwidth and readily detecting some types of electromagnetic interference (EMI) [5]. Typically the two streams of sampled data from each sensor are converted to the frequency domain by FFT, multiplied together to form the cross-spectrum, averaged over many datasets to produce a smooth cross-spectrum and then used to form a ratio with the cross-spectrum from the other sensor. Thus, conceptually, each bin of the ratio spectrum formed from the cross-spectra can be treated as a noise thermometer with a bandwidth corresponding to the width of the FFT bins.

For several years, NIST has been developing a switching-correlator type noise thermometer that uses a synthetic-noise source based on a Josephson ac-voltage generator [6–12]. The synthetic source replaces the sensing resistor at the reference temperature, as shown in figure 2. The NIST project was motivated by two factors. Firstly, with conventional noise thermometers there is a requirement to match the noise powers of the two sensors to minimize the influence of non-linearities within the correlator [13]. This means the sensing resistances must be related according to $R(T)T = R(T_0)T_0$ (see (1)). At the same time it is desirable to match the sensing resistances, $R(T) = R(T_0)$, in order to minimize differences in frequency response of the transmission lines connecting the sensors to the preamplifiers [14, 15]. In the conventional design, both requirements cannot be satisfied simultaneously. The use of a synthetic-noise source in place of the measurement at T_0 enables both the noise powers and the source resistance to be matched independently.

The second motivational factor for the new noise thermometer was the possibility of determining Boltzmann’s constant. With the 2005 announcement of the Comité International des Poids et Mesures to consider updating the SI so all the base units of the SI are defined in terms of fundamental physical constants [16], this motivating factor has increased in importance.

The NIST quantized voltage noise source (QVNS) produces pseudo-random noise based on a comb of frequencies of constant amplitude and random phase [6]. The main purpose of this paper is to investigate the requisite properties of the frequency comb. First we briefly summarize the rationale for using the synthetic-noise source. This is followed by analyses identifying matching criteria for the source. The criteria relate to the number of tones in the frequency comb, and principally,

the spacing between the tones. First we demonstrate in detail the limitations of conventional noise thermometers.

2. Matching criteria in conventional noise thermometers

2.1. Matching of the noise powers

Amongst the many systematic errors that affect noise thermometers, non-linearity is a major problem. The input signals (equation (1)) are of the order of $1 \mu\text{V}$ rms, so that each channel of the correlator requires an overall voltage gain of the order of 10^6 to obtain a voltage suitable for analogue-to-digital conversion. The problem of keeping distortion products below 0.001% with JFET preamplifiers operated without feedback [15], multiple amplifier and filter stages and high-speed analogue-to-digital converters [17, 18], is practically impossible to solve. The only practical approach is to control how the errors propagate, and this usually necessitates the matching of the various contributions to the noise signals.

Suppose the (amplitude) transfer function for each channel of the correlator, when referred to the correlator input, is represented as the Taylor series [13, 19]

$$V_j = \sum_{k=0}^{\infty} a_{jk}(V_T + V_{n_j})^k, \quad a_{j1} = 1, \quad (3)$$

where the index j indicates the channel number ($j = 1, 2$), the index k indicates the order of the coefficient and V_{n_j} is the equivalent input noise voltage for channel j . The coefficients a_{j0} therefore represent the offset voltages and a_{j1} represent the linear gains. All of the a_{jk} except a_{j1} represent the unwanted non-linear terms and are assumed to be small.

When the signals from the two correlator channels are multiplied and averaged we obtain the measured noise power

$$\begin{aligned} \overline{V_T^2(T)}_{\text{meas}} = & a_{10}a_{20} + a_{10}a_{22}\sigma_{n_2}^2(T) + a_{20}a_{12}\sigma_{n_1}^2(T) \\ & + a_{12}a_{22}\sigma_{n_1}^2(T)\sigma_{n_2}^2(T) + \sigma_T^2(T)(1 + a_{10}a_{22} + a_{12}a_{20} \\ & + \sigma_{n_1}^2(T)(a_{12}a_{22} + 3a_{13}) + \sigma_{n_2}^2(T)(a_{12}a_{22} + 3a_{23}) \\ & + 9a_{13}a_{23}\sigma_{n_1}^2(T)\sigma_{n_2}^2(T) + 3\sigma_T^4(T)(a_{13} + a_{23} \\ & + a_{12}a_{22} + \sigma_{n_2}^2(T) + \sigma_{n_1}^2(T))3a_{13}a_{23} + \dots, \end{aligned} \quad (4)$$

where $\sigma_T^2(T) = \overline{V_T^2(T)}$ is the variance of the thermal noise signal (total noise power), $\overline{V_T^4} = 3\sigma_T^4(T)$, as expected for a Gaussian variable, and $\overline{V_{n_j}^2(T)} = \sigma_{n_j}^2(T)$. Note that all of the even-order non-linearity coefficients ($a_{j0}, a_{j2}, a_{j4}, \dots$) occur in (4) only as products of two small non-linear terms. However, some of the odd-order non-linearity coefficients (a_{j3}, a_{j5}, \dots) appear in terms that are first order in the coefficients and therefore probably contribute greater error in the correlator output. Additionally, it is possible to eliminate the even-order non-linearities completely by commutating the preamplifier inputs [19].

To simplify the analysis we consider only the most significant odd-order terms of (4) (the conclusions from the analysis do not change if more terms are added):

$$\begin{aligned} \overline{V_T^2(T)}_{\text{meas}} \approx & \sigma_T^2(T) + 3(a_{13} + a_{23})\sigma_T^4(T) \\ & + 3[a_{13}\sigma_{n_1}^2(T) + a_{23}\sigma_{n_2}^2(T)]\sigma_T^2(T). \end{aligned} \quad (5)$$

The expected ratio of two noise-power measurements made at different temperatures is therefore

$$\frac{\overline{V_T^2(T)}_{\text{meas}}}{\overline{V_T^2(T_0)}_{\text{meas}}} \approx \frac{\sigma_T^2}{\sigma_{T_0}^2} \{1 + 3(a_{13} + a_{23})[\sigma_T^2(T) - \sigma_T^2(T_0)] + 3a_{13}[\sigma_{n1}^2(T) - \sigma_{n1}^2(T_0)] + 3a_{23}[\sigma_{n2}^2(T) - \sigma_{n2}^2(T_0)]\}. \quad (6)$$

Thus the error in the measured noise-power ratio due to the non-linearities increases in proportion to the differences in the various noise powers (the terms in square brackets). The criteria for eliminating the non-linearity errors are

$$\sigma_T^2(T) = \sigma_T^2(T_0) \quad (7)$$

and

$$\sigma_{n1}^2(T) = \sigma_{n1}^2(T_0) \quad (8a)$$

and

$$\sigma_{n2}^2(T) = \sigma_{n2}^2(T_0). \quad (8b)$$

The criterion for the correlated noise, (7), applied to (1) leads to the equivalent requirement $R(T)T = R(T_0)T_0$, and hence a different sensing resistor or reference resistor must be chosen for each temperature measured. Because the amplifier noise is common to both sensors, the mismatches in the uncorrelated noises arise from small differences in the series resistance of the components in the transmission lines. The matching criteria for the uncorrelated noises (8a) and (8b) can be satisfied simply by inserting low-value resistors into some of the input connections to the switch.

2.2. Matching of the transmission lines

Ideally, and for sufficiently narrow FFT bins, the power in each bin of the averaged cross-spectra converges on a value proportional to the power spectral density of the amplified sensor signal times the bandwidth of the bin (i.e. independent of preamplifier noise currents and voltages). The measured power in the FFT bin at frequency f is

$$\overline{V_R^2(T, f)} = 4kTR(T)F |H_R(R(T), f)|^2 |A(f, T)|^2, \quad (9)$$

where F is the bandwidth of each FFT bin, H_R is the frequency response of the transmission line connecting the sensor to the preamplifiers and A is the frequency-dependent gain of the amplifiers and filters in the noise thermometer. Note that H_R is dependent on the sensor resistance. The ratio of the measured powers at two temperatures is

$$\frac{\overline{V_R^2(T, f)}}{\overline{V_R^2(T_0, f)}} = \frac{TR(T) |H_R(R(T), f)|^2}{T_0R(T_0) |H_R(R(T_0), f)|^2}, \quad (10)$$

which is independent of the amplifier frequency response. Ideally the ratio of the remaining two frequency responses is unity so that (2) follows. However, if the two transmission lines are nominally identical, so they have the same inductance and capacitance, the ratio of the frequency responses depends on the sensor resistance that terminates the lines [15]

$$\frac{|H_R(R(T), f)|^2}{|H_R(R(T_0), f)|^2} = 1 + 4\pi^2 f^2 (C_t + 2C_{in})^2 \times [R(T_0)^2 - R(T)^2], \quad (11)$$

where C_t and C_{in} are, respectively, the transmission line and preamplifier input capacitances. Thus the condition for zero error due to the differences in the transmission-line frequency responses is

$$R(T) = R(T_0), \quad (12)$$

which is in direct conflict with the linearity matching requirement of (7).

Note that the transmission-line inductance does not appear in (11). Although a factor in the frequency response of the transmission line, the inductance appears only in high-order terms in combination with the capacitances, which do not normally change significantly between the two measurements.

Unlike the case for the non-linearity errors, there are alternative means for managing the transmission-line errors. Ideally, the capacitances or inductances of the transmission lines are adjusted so that the characteristic impedance of each line is matched to its sensor resistance [14]. This ensures that the frequency response of each transmission line is as wide and as flat as practical. The matching criterion for the characteristic impedance is

$$R^2 = \frac{L(2C_{in} + C_t)}{(C_{in} + C_t)^2}. \quad (13)$$

Normally the sensing resistance is greater than the characteristic impedance of the transmission line so a small series inductance is required to achieve the match.

Historically, it was accepted practice to match only the RC time constants by adding capacitance to one of the transmission lines [20]. However, this practice neglects the stray inductance and results in an even larger error due to the interaction of the inductance and capacitance [15]. A variation on this approach is to shunt one of the transmission lines with additional capacitance so that the ratio of the two cross-spectra is as flat as practical [10, 11]. This achieves the desired result of a good match of frequency responses at low frequencies, but the high-order terms due to the interaction of inductance and capacitance are still large and limit the available bandwidth.

It is also possible to measure the combined capacitance of the transmission line, switch capacitance and the preamplifier input capacitance, and to calculate a correction using (11) [21]. This requires impedance measurements to be made while the preamplifier is live. Additionally, the measurements may give different values for different positions of the switch.

Because the transmission-line error increases as frequency squared, the uncertainty in corrections or the uncertainty in the match of the transmission lines also increases as frequency squared. This is one of the main factors limiting the useful bandwidth of the noise thermometer.

3. The rationale for a synthetic-noise source

The NIST QVNS is a delta-sigma digital-to-analogue converter. It uses first-order oversampling techniques to produce a sequence of pulses at a very high frequency with the required baseband (typically 0–4 MHz) waveform of interest

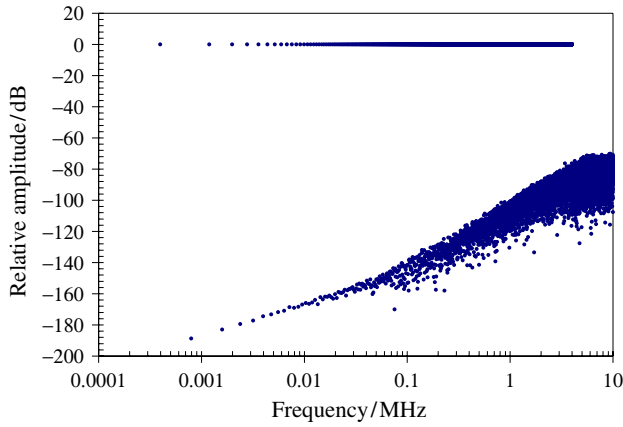


Figure 3. The first 10 MHz of the QVNS spectrum calculated from a code sequence with a pattern repetition frequency of 400 Hz. The upper branch shows the odd harmonics up to 4 MHz. The lower branch shows the even harmonics up to 4 MHz and all harmonics above 4 MHz. The amplitudes of the even harmonics are indicative of the accuracy of the code.

[22]. The advantage of the Josephson system is that each pulse has quantized area [23]

$$\int V(t) dt = nh/2e, \quad (14)$$

where n is an integer (normally $n = 1$ in the NIST QVNS), h is Planck’s constant and e is the charge of the electron. Thus, the synthesized voltage can be calculated exactly from the known sequence of pulses, the clock frequency of the pulse generator and fundamental physical constants.

The matching resistors used to terminate the QVNS transmission line are placed in the leads of the transmission line (figure 2) so that they produce only uncorrelated noise. The resistors are also maintained at 4 K so they do not unduly increase the uncorrelated noise.

The QVNS uses a continuously recycled digital code that is M bits long, giving the synthesized waveform a power spectrum composed of a series of tones (harmonics) at multiples of the pattern repetition frequency, $f_1 = f_S/M$, where f_S is the clock frequency of the code generator, typically 10 GHz [6]. Software is used to generate the code sequence to produce the desired waveform. For the noise thermometer, the usual waveform is a series of tones at the *odd* harmonics $f_1, 3f_1, 5f_1, \dots$, all of the same amplitude but random phase. This yields a pseudo-random noise waveform with a calculable power spectral density, as shown in figures 3 and 4.

The amplitudes of the tones are chosen so that the average power spectral density of the synthesized noise is the same as that of the noise from the sensing resistor of the noise thermometer. The average power of a QVNS tone located at f_i , as measured by the correlator, is

$$\overline{V_{QVNS}^2(T, f_i)} = NFv_{\text{calc}}^2(T)|H_{QVNS}(R_{QVNS}, f_i)|^2|A(f_i, T)|^2, \quad (15)$$

where $v_{\text{calc}}(T)$ is the average power spectral density calculated from the code sequence, the clock frequency, and $N = 2f_1/F$

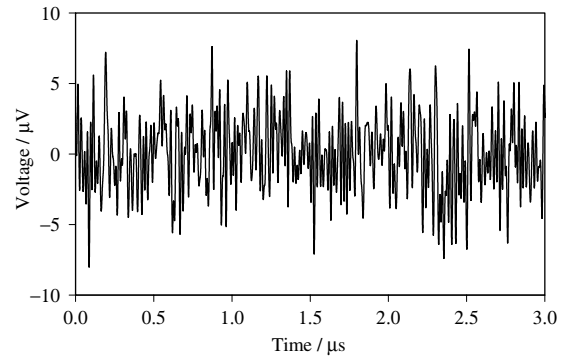


Figure 4. A 3 μs sample of the calculated QVNS output signal showing the noise-like waveform.

is the number of FFT bins separating each *odd* tone. We refer below to this collection of N bins as a ‘block’. In order to ensure that N is an integer, specific pattern lengths are required for the Josephson waveform; the clock frequencies of the analogue-to-digital converters and the code generator are chosen to be commensurate; and they must use a common 10 MHz reference. In (15), R_{QVNS} is the resistance of the series resistors terminating the QVNS transmission line (figure 2). A detailed description of the principles of the noise source and the electronic design considerations can be found in [6,7,9,23].

3.1. Relative temperature measurements

When the thermometer is used in relative mode, it makes two separate measurements of noise-power ratio [8]. In the first measurement at temperature T , the following ratio is calculated for each block:

$$\frac{\overline{V_R^2(T, f_i)}}{V_{QVNS}^2(T, f_i)} = \frac{4kTR(T)}{v_{\text{calc}}^2(T)} \times \frac{\sum_{n=(1-N)/2}^{(N-1)/2} |A(f_i + nF, T)|^2 |H_R(R(T), f_i)|^2}{N |A(f_i, T)|^2 |H_{QVNS}(R_{QVNS}, f_i)|^2}. \quad (16)$$

The numerator includes the sum of the measured sensor noise powers from the block of N FFT bins located about the QVNS tone, and the denominator includes the measured power in the tone itself. Note that $v_{\text{calc}}(T)$ is chosen so that the noise-power ratio is very close to unity and the effects of non-linearities are negligible.

If it is assumed that the frequency response of the transmission lines and amplifiers is constant over the narrow bandwidth covered by one block of FFT bins, (16) simplifies to

$$\frac{\overline{V_R^2(T, f_i)}}{V_{QVNS}^2(T, f_i)} = \frac{4kTR(T)}{v_{\text{calc}}^2(T)} \frac{|H_R(R(T), f_i)|^2}{|H_{QVNS}(R_{QVNS}, f_i)|^2}, \quad (17)$$

which is independent of the amplifier response. If a second noise-power-ratio measurement is made at the reference temperature, T_0 , using exactly the same sensor and transmission line as for (17), the unknown temperature calculated from the noise powers associated with the i th QVNS

tone is

$$T(f_i) = T_0 \frac{R(T_0) \overline{V_{\text{QVNS}}^2(T_0, f_i)}}{R(T) \overline{V_{\text{QVNS}}^2(T, f_i)}} \frac{\overline{V_R^2(T, f_i)}}{\overline{V_R^2(T_0, f_i)}} \times \frac{|H_R(R(T_0), f_i)|^2 v_{\text{calc}}^2(T)}{|H_R(R(T), f_i)|^2 v_{\text{calc}}^2(T_0)}. \quad (18)$$

This expression is computed for each QVNS tone and all such measured temperatures are averaged to give the final measurement.

Note that the frequency response of the transmission line for the synthetic source is absent from (18). By using the same sensor and transmission line for both of the measurements leading to (18), we ensure, by design, that the first four ratios in (18) are all very close to 1.0. Only the last ratio, $v_{\text{calc}}^2(T)/v_{\text{calc}}^2(T_0)$, differs significantly from unity, but it is calculated with negligible uncertainty from fundamental constants and the pulse-generator frequency. The use of the QVNS enables the thermometer to operate with the same sensing resistance, the same transmission line and the same noise powers, therefore overcoming the matching conflict inherent in conventional noise thermometers.

3.2. Absolute temperature measurements

In absolute mode, the temperature is inferred from (17) directly in terms of fundamental constants:

$$T(f_i) = \frac{v_{\text{calc}}^2(T) \overline{V_R^2(T, f_i)}}{4kR(T) \overline{V_{\text{QVNS}}^2(T, f_i)}} \frac{|H_{\text{QVNS}}(R_{\text{QVNS}}, f_i)|^2}{|H_R(R(T), f_i)|^2}. \quad (19)$$

Note that all terms are ratios of similar quantities, the ratio of two calculated quantities (one with a measured resistance), two measurements of noise power and the ratio of two frequency responses. Although the matching of the frequency responses remains difficult, there is no longer a constraint to have resistances of a particular value, and they can be chosen to be matched to the line. This maximizes the bandwidth of the system and minimizes the frequency-response error. Further discussion of this point is beyond the scope of this paper but we note that the remnant second-order effects of the transmission-line mismatch can be addressed by extrapolating the measured temperature to zero frequency [11].

By making the measurements at the triple point of water, (19) can be used to find a value for k , Boltzmann's constant. This requires a good ac measurement of the resistance of the sensor and the measurement of the ratio of the noise powers. Note that making a Boltzmann constant determination directly from (1) using conventional noise thermometers involves the practically impossible tasks of characterizing the gain and bandwidths of the noise thermometer [24]. The shift to processing in the frequency domain to eliminate the analogue filter response and the use of a source with calculable power spectral density makes the measurement possible. Determining k from (19) effectively involves the balancing of power spectral densities rather than noise powers. The near perfect linearity in both frequency and amplitude of the QVNS synthesized waveforms makes the determination of k possible.

4. Matching criteria in a noise thermometer with the QVNS

4.1. Noise-power matches

The noise-power matches for the synthetic-noise source are exactly the same as for a conventional noise thermometer (equations (7), (8a) and (8b)). However, because the impedance-matching resistors are inserted into the leads of the transmission line and operate at a temperature near 4 K, they also produce uncorrelated noise, so making an additional contribution to the uncorrelated noises, which must be considered.

4.2. Impedance matching

In principle, the use of the QVNS allows the simultaneous matching of the noise powers and the resistors terminating the transmission line. However, the situation is not as simple as might at first be thought. In figure 1 a single resistor terminates the two transmission lines connecting the sensor to each preamplifier. In figure 2, the short circuit of the Josephson junctions effectively decouples the two pairs of leads to the preamplifiers. This means that, for otherwise identical transmission lines (same stray inductances and capacitances), the total resistance inserted into each pair of the QVNS lines must be twice the sensor resistance (i.e. each lead resistor shown in figure 2 must be equal to the sensing resistance shown in figure 1). In practice, the QVNS and sensor transmission lines will be different, so the ratios of the terminating resistances will not be exactly 2 : 1. Currently, for the NIST QVNS, the terminating resistance is about 1.6 times the sensing resistance.

4.3. Voltage-distribution match

The requirement to consider the number of spectral elements (tones) in the QVNS frequency comb is motivated by the need to ensure that the distortion products in the thermal noise signal and the QVNS signal are the same. If it is assumed that the QVNS produces a sine wave of the same total power as the thermal signal; then the first-order distortion-product terms of (4) give rise to a noise power at the output of the correlator of

$$\overline{V_1 V_2}|_{\text{sin}} = \sigma_T^2 + \frac{3}{2}(a_{13} + a_{23})\sigma_T^4 + 3(a_{13}\sigma_{n1}^2 + a_{23}\sigma_{n2}^2)\sigma_T^2. \quad (20)$$

The difference between the correlator output (20) for the sine wave and (5) for the Gaussian noise arises because the fourth moment of the distribution of voltages for a sine wave is different from that for Gaussian noise (when the two have the same second moment). Thus it is not possible to use a pure sine wave as a reference signal without incurring errors from the non-linearity effects. If the full Taylor-series expansion of the correlator transfer function is considered, then all of the non-zero statistical moments of the signal distribution will be manifest in (4). Therefore, for the QVNS reference waveform to achieve a good match against the noise in the presence of non-linearity, the distribution for the QVNS waveform must have the same statistical moments as that of the noise

Table 1. The first four non-zero moments of the distributions for a single sinusoid, m sinusoids and a Gaussian signal.

Moment	Moment for single sinusoid	Moment for m sinusoids	Moment for Gaussian
μ_2	σ_T^2	σ_T^2	σ_T^2
μ_4	$\frac{3}{2}\sigma_T^4$	$\left(3 - \frac{3}{2m}\right)\sigma_T^4$	$3\sigma_T^4$
μ_6	$\frac{5}{2}\sigma_T^6$	$\left(15 - \frac{45}{2m} + \frac{10}{m^2}\right)\sigma_T^6$	$15\sigma_T^6$
μ_8	$\frac{35}{8}\sigma_T^8$	$\left(105 - \frac{315}{m} + \frac{1435}{4m^2} - \frac{1155}{8m^3}\right)\sigma_T^8$	$105\sigma_T^8$

signal, i.e. the distribution of voltages comprising the QVNS waveform must be Gaussian.

The argument above is based on a Taylor-series approximation of the amplitude dependence of distortion-producing components. There are other distortion mechanisms associated with the analogue-to-digital-converters [17, 18] and slew-rate limiting that can also produce distortion that is not well described by Taylor series. However, a synthetic reference that has all of the same moments and spectral distribution as Gaussian noise will produce the same distortion products as the noise.

In order to calculate the distribution for the probability density distribution for many sinusoids, consider first the distribution for a single sinusoid of amplitude A :

$$p(x) = \frac{1}{\pi\sqrt{A^2 - x^2}} \quad \text{for } -A < x < A$$

$$= 0 \quad \text{for } |x| > A. \quad (21)$$

The probability density function for a collection of N such sinusoids, all of the same amplitude and random phase, is obtained by convolving the probability density function (21) with itself many times. The convolution is more easily computed in the Fourier domain by the use of the characteristic function (Fourier transform) of the distribution [25]:

$$F_x(\xi) = \int_{-\infty}^{+\infty} p(x) \exp(i\xi x) dx = J_0(A\xi), \quad (22)$$

where $J_0(A\xi)$ is a Bessel function of the first kind. The n th moment, μ_n , of the distribution (21), $p(x)$, is obtained by differentiating (22) n times according to [25]

$$\mu_n = \langle x^n \rangle = (-i)^n \frac{d^n}{d\xi^n} F_x(\xi) \Big|_{\xi=0}. \quad (23)$$

Since convolution in the x -domain is equivalent to multiplication in the ξ -domain, the moments of the distribution of the sum of m statistically independent sinusoids (with random phase) is also given by (23), but with $F_x(\xi)$ replaced by $F_x^m(\xi)$. The results of the calculation, which was carried out with an algebraic mathematics application, are summarized in table 1. The amplitude of the m sinusoids has been chosen so that the total mean-square power is always σ_T^2 . Note that the odd moments for all of the distributions are zero because the distributions are symmetric about zero.

Table 1 shows that as the number of sinusoids increases, the moments all converge to the values for the Gaussian

distribution. The convergence is expected since this is an example of the central limit theorem [25]. Secondly, and most importantly, the convergence improves as $1/m$.

The $1/m$ convergence of the frequency comb to a Gaussian distribution gives a general guide for the design of the QVNS. For example, in a noise thermometer with the total distortion below 0.1% of the noise power, a synthetic spectrum comprising 1000 or more sinusoids should ensure that the differences in distortion products are below the parts-per-million level. However, the spectral distribution of the sinusoids must also be considered. To match the distortion products exactly, the total noise powers must be matched (equations (7) and (9)) at every stage of the noise thermometer. The only way to achieve this is for the frequency comb to extend to the full bandwidth of the preamplifier. Since about 1000 tones are required within the nominal passband of the thermometer, which is usually much less than the bandwidth of the preamplifier, the total number of tones required may be very much greater than 1000. Experimentally, we have observed no differences in correlator output when the bandwidth of the tones is changed from 4 MHz to 8 MHz, indicating no measurable bandwidth-related non-linearity in the measurement system.

A reference waveform based on a non-constant power spectral density could also be considered. It could, for example, be synthesized from a frequency comb with Rayleigh distributed amplitudes, as is characteristic of narrow-band noise [25]. However, this option probably converges to a Gaussian distribution more slowly than the equi-amplitude sinusoids as described above. If we consider the case for two sinusoids this becomes clear. Clearly if the amplitudes of the two sinusoids are very much different, the improvement in statistics will be only marginally better than having one large-amplitude sinusoid. The best situation must be when the two sinusoids have equal amplitudes. This must also apply when there are many sinusoids.

4.4. Spectral match

The synthetic noise generated by the QVNS is not uniformly distributed throughout the spectrum, but distributed as evenly spaced tones of equal amplitude such that the average power spectral density of the thermal noise signal and the QVNS are the same. In the noise thermometer operated at NIST, the signals are sampled by a fast analogue-to-digital converter,

with the data-acquisition period chosen so that each bin in the FFT is approximately 1 Hz wide. Ideally, the QVNS would generate tones at 1 Hz intervals so that the averages of the two power spectra are indistinguishable. However, as discussed above, the tone spacing is limited by the memory of the code generator driving the QVNS. When the thermometer is operating in absolute mode, this leads to an error that is dependent on the frequency response of the amplifiers and filters.

If it is assumed that the frequency response of the transmission lines is constant over the block of N bins, but the amplifier response is not constant, then the measured noise power ratio (16) is

$$\frac{V_R^2(T, f_i)}{V_{\text{QVNS}}^2(T, f_i)} = \frac{4kTR(T)}{v_{\text{calc}}^2(T)} \frac{|H_R(R(T), f_i)|^2}{|H_{\text{QVNS}}(R_{\text{QVNS}}, f_i)|^2} \times \frac{\sum_{n=(1-N)/2}^{(N-1)/2} |A(f_i + nF, T)|^2}{N |A(f_i, T)|^2}. \quad (24)$$

Equation (24) shows the approximation leading to (17) is based on the assumption that

$$\frac{1}{N} \sum_{n=(1-N)/2}^{(N-1)/2} |A(f_i + nF, T)|^2 = |A(f_i, T)|^2, \quad (25)$$

i.e. the frequency response of the thermometer at the frequency of the tone is equal to the average frequency response over the whole block. Note that it is assumed that the QVNS tone is in the centre of the block. Where the frequency response of the filter is relatively constant (actually trapezoid), (25) proves to be a good approximation. However, near the edges of the pass band of the thermometer, where the frequency response is curved, the approximation becomes worse.

The accuracy of the block summations can be evaluated by noting that the discrete sum (25) has a continuous analogue:

$$\frac{1}{2f_1} \int_{f_i-f_1}^{f_i+f_1} |A(f)|^2 df = |A(f_i)|^2. \quad (26)$$

If $A(f)$ has an n -pole low-pass Butterworth response with a 3 dB cutoff frequency of f_0 , then the integrand of (26) can be expanded as a Taylor series about f_i to give

$$|A(f)|^2 \approx \frac{f_0^{2n}}{f_0^{2n} + f_i^{2n}} - \frac{2nf_0^{2n} f_i^{2n-1}}{(f_0^{2n} + f_i^{2n})^2} (f - f_i) + \frac{nf_0^{2n} f_i^{2n-2} ((2n+1)f_i^{2n} - (2n-1)f_0^{2n})}{(f_0^{2n} + f_i^{2n})^3} (f - f_i)^2, \quad (27)$$

and hence the value for the integral (26) is

$$\frac{1}{2f_1} \int_{f_i-f_1}^{f_i+f_1} |A(f)|^2 df \approx |A(f_i)|^2 \times \left[1 + \frac{n}{12} \frac{f_i^{2n}}{f_i^2} \frac{((2n+1)f_i^{2n} - (2n-1)f_0^{2n})}{(f_0^{2n} + f_i^{2n})^2} \frac{4f_1^2}{f_i^2} \right]. \quad (28)$$

Equation (28) shows that the relative accuracy of the approximations, (25) and (26), diverges as the square of the

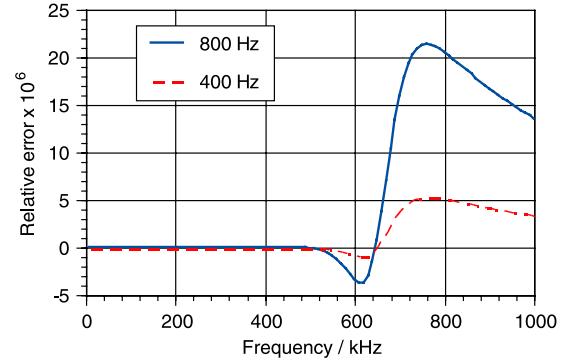


Figure 5. The error in the block summation for tone spacing of 400 Hz and 800 Hz. It is assumed that the noise thermometer has an 11-pole low-pass Butterworth response with a cutoff frequency of 650 kHz.

block bandwidth (equal to the tone spacing) and roughly as the square of the number of poles in the response of the filter. The relative error due to the approximation is given by the second term in the square brackets of (28). At frequencies well above the cutoff frequency of the filter, the error has a $1/f_i^2$ dependence.

In the NIST thermometer, we recently reduced the measurement bandwidth of our electronics from 2 MHz to 650 kHz by replacing the active four-pole Butterworth anti-alias filter [7] with a passive 11-pole low-pass Butterworth filter. $A(f)$ is dominated by the response of this anti-aliasing filter. The relative error is plotted in figure 5 for two values of tone spacing, 400 Hz and 800 Hz. The most notable feature of the curves is that the most serious effects are apparent only above the cutoff frequency of the filter, and the effects are practically negligible at frequencies below 500 kHz. Note too, the zero in the error near the cutoff frequency; this is also apparent from (28).

The linear term of (27) also provides the sensitivity of the integration to errors in the location of the tone frequency. This is an issue because the fastest and most frequently used FFTs are based on 2^n -radix algorithms, and hence there is always an even number of FFT bins per tone. Additionally, for the NIST QVNS the tone spacing is twice the pattern repetition frequency of the QVNS. This means that N , the number of bins per tone, is always an even number, and there is no FFT bin exactly centred between two tones. (In the summations of (17), (24) and (25) N is assumed to be odd to avoid having to raise this point before now.) The nearest tone is located 0.5 of an FFT bin from the centre of the summed FFT bins. If the tone is located at f_i and the block summation is centred on f_c then the result of the block summation is

$$\frac{1}{2f_1} \int_{f_c-f_1}^{f_c+f_1} |A(f)|^2 df \approx |A(f_i)|^2 \times \left[1 + 2n \frac{f_c^{2n}}{(f_0^{2n} + f_c^{2n})} \frac{(f_c - f_i)}{f_c} \right]. \quad (29)$$

The second term in the square brackets of (29) gives the relative error in the block summation due to the offset of the tone from the block centre. Note that the error term has the shape of a

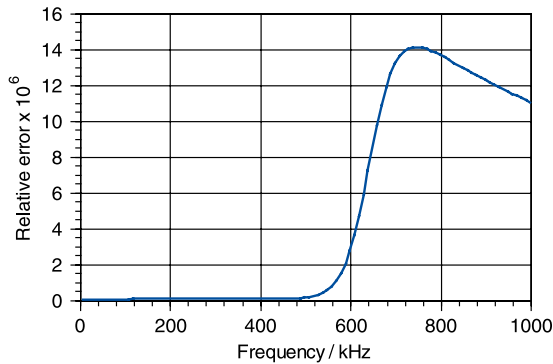


Figure 6. The error in the block summations with the tone misplaced from the block centre by 0.5 Hz. The filter has an 11-pole low-pass Butterworth response with a cutoff frequency of 650 kHz.

high-pass filter multiplied by $1/f_c$. This yields little error at low frequencies and a $1/f$ shape above the cutoff frequency of the filter. This is plotted in figure 6 for a 0.5 Hz offset and an 11-pole low-pass Butterworth filter with a cutoff frequency at 650 kHz. Note again that there is practically no error for frequencies below 500 kHz, and the error is greatest near the band edge.

There are at least three possible approaches to managing the block summation error caused by the tone offset. Firstly, ignore it and consider only data below about 500 kHz (approximately $0.75f_0$). However, it is desirable to remove all such spectral artefacts to avoid complicating the matching of the transmission lines. Secondly, because the effect is linear, it can be eliminated by alternating the block summations so that the 0.5 Hz offset is alternately positive and negative. Thirdly, a value for the expected amplitude of a tone located at the true centre of the block can be obtained by interpolating between the neighbouring-tone amplitudes. At NIST we have adopted the latter approach using a cubic spline to carry out the interpolation.

5. Conclusions

A noise thermometer using a synthetic-reference-noise source overcomes the conflicting sensor-matching requirements that afflict conventional noise thermometers. Additionally, a noise thermometer using a Josephson ac-voltage generator to synthesize a noise waveform consisting of a frequency comb of known power spectral density offers a means for determining Boltzmann's constant.

In order to mitigate distortion effects in the correlator, the synthetic-noise source must produce a signal that closely approximates a Gaussian voltage distribution. This ensures that all of the various distortion products (effectively the moments of the distribution of voltages) are the same for both the sensor signal and the synthetic noise. For a pseudo-random noise signal composed of a frequency comb with m sinusoids of constant amplitude and random phase, the moments of the distribution of sinusoids converge to the Gaussian moments as $1/m$. Thus, for a noise thermometer with about 0.1% distortion, a minimum of 1000 sinusoids are required within

the thermometer pass band to ensure that the effects are below the part-per-million level.

Due to the limited memory available in the code generator, it is not possible to produce tones for every FFT bin of the processed signal. Consequently, if the frequency response of the noise thermometer is not constant, the noise thermometer response at the tone frequency may not be representative of the response over the block of FFT bins near the tone. Near the edges of the thermometer pass band, this will cause errors proportional to the square of the tone spacing. A similar error occurs if there is an offset between the tone and the centre of the block between two tones.

In total there are six constraints on a noise thermometer using a frequency comb as a synthetic reference. The first three constraints are the same as for conventional noise thermometers.

- (i) To avoid errors due to correlator non-linearity, the amplitude of the synthetic noise must be the same as that of the thermal noise signal.
- (ii) The uncorrelated noise powers in each channel must be the same for the two measurements. In combination with (i), this means the total noise powers in each channel must be the same for both measurements. Note that the synthetic-noise source has additional noise due to extra resistors terminating the transmission line.
- (iii) To maximize bandwidth and minimize transmission-line errors, the resistances terminating the sensor and synthetic source transmission lines should be terminated by a resistor of the characteristic impedance of the line.

The second group of three constraints relate specifically to a synthetic-noise source based on the frequency comb.

- (iv) To minimize the effects of non-linearity, the synthetic-noise source must generate a large number of tones across the full spectrum of the noise thermometer to ensure the sensor noise and synthetic noise have the same statistical moments.
- (v) The spacing of the tones from the synthetic source must be small enough to ensure accurate block summations of the spectral power.
- (vi) Each tone should be at the centre of each spectral block used to calculate the ratio spectrum, or measures taken during computations to compensate for any offset.

Acknowledgments

The authors gratefully acknowledge the contributions of Charles Burroughs, Paul Dresselhaus, Sae Woo Nam, Horst Rogalla and Wes Tew to useful discussions and for assistance with the development of the QVNS and the noise thermometer.

References

- [1] Brixy H 1971 Temperature measurement in nuclear reactors by noise thermometry *Nucl. Instrum. Methods* **97** 75–80

- [2] Brixy H, Hecker R, Oehmen J, Rittinghaus K F, Setiawan W and Zimmermann E 1982 Noise thermometry for industrial and metrological applications at KFA Jülich *Temperature: its Measurement and Control in Science and Industry* vol 6, ed J F Schooley (New York: American Institute of Physics) pp 129–31
- [3] Fink H J 1959 A new absolute noise thermometer at low temperatures *Can. J. Phys.* **37** 1397–406
- [4] White D R *et al* 1996 The status of Johnson noise thermometry *Metrologia* **33** 325–35
- [5] Willink R and White D R 1998 Detection of corruption in Gaussian processes with application to noise thermometry *Metrologia* **35** 787–98
- [6] Benz S P, Dresselhaus P D and Martinis J 2003 An ac Josephson source for Johnson noise thermometry *IEEE Trans. Instrum. Meas.* **IM-52** 545–9
- [7] Nam S, Benz S, Dresselhaus P D, Tew W L, White D R and Martinis J 2003 Johnson noise thermometry measurements using a quantized voltage noise source for calibration *IEEE Trans. Instrum. Meas.* **IM-52** 550–4
- [8] Nam S W, Benz S P, Martinis J M, Dresselhaus P D, Tew W L and White D R 2003 A ratiometric method for Johnson noise thermometry using a quantized voltage noise source *Temperature: its Measurement and Control in Science and Industry* vol 7, ed D C Ripple (New York: American Institute of Physics) pp 37–42
- [9] Benz S P, Martinis J M, Nam S W, Tew W L and White D R 2002 A new approach to Johnson noise thermometry using a Josephson quantized voltage source for calibration *Proc. TEMPMEKO 2001* ed B Fellmuth *et al* (Berlin: VDE Verlag) pp 37–44
- [10] Nam S, Benz S, Dresselhaus P, Burroughs C, Tew W L, White D R and Martinis J M 2005 Progress on Johnson noise thermometry using a quantum voltage noise source for calibration *IEEE Trans. Instrum. Meas.* **IM-54** 653–7
- [11] Labenski J R, Tew W L, Nam S W, Benz S P, Dresselhaus P D and Burroughs C J 2007 Resistance-based scaling of noise temperatures from 1 kHz to 1 MHz *IEEE Trans. Instrum. Meas.* **IM-56** 481–5
- [12] Tew W L, Labenski J R, Nam S W, Benz S P, Dresselhaus P D and Burroughs C J 2007 Johnson noise thermometry near the zinc freezing point using resistance-based scaling *Int. J. Thermophys.* **28** 629–45
- [13] Klein H-H, Klempt G and Storm L 1979 Measurement of the thermodynamic temperature of ^4He at various vapour pressures by a noise thermometer *Metrologia* **15** 143–54
- [14] Höwener H 1986 Noise thermometry in nuclear power plants. A contribution to signal transmission of broad band spectra in noise thermometry, Kernforschungsanlage Jülich GmbH, Institut für Reaktorentwicklung
- [15] White D R and Zimmermann E 2000 Pre-amplifier limitations on the accuracy of Johnson noise thermometers *Metrologia* **37** 11–23
- [16] Recommendation 1 (CI 2005): Preparative steps towards new definitions of the kilogram, the ampere, the kelvin and the mole in terms of fundamental constants (CIPM, Sèvres, 2005)
- [17] White D R and Pickup C P 1987 Systematic errors in digital cross-correlators due to quantisation and differential nonlinearity *IEEE Trans. Instrum. Meas.* **IM-36** 47–53
- [18] White D R 1992 Calibration of a digital cross-correlator for Johnson noise thermometry *Metrologia* **29** 23–35
- [19] White D R and Mason R S 2004 An emi test for Johnson noise thermometry *Proc. TEMPMEKO 2004 (Faculty of Mechanical Engineering and Naval Architecture, Zagreb)* ed D Zvizdic *et al* pp 485–90
- [20] Pickup C P 1975 A high-resolution noise thermometer for the temperature range 90–100 K *Metrologia* **11** 151–9
- [21] White D R, Mason R S and Saunders P 2001 Progress towards a determination of the indium freezing point by Johnson noise thermometry *Proc. Tempmeko 2001* ed B Fellmuth *et al* (Berlin: VDE Verlag) pp 129–34
- [22] Candy J C 1997 An overview of basic concepts *Delta-Sigma Data Converters: Theory, Design, and Simulation* ed S R Norsworthy *et al* (Piscataway, NJ: IEEE)
- [23] Benz S P and Hamilton C A 1996 A pulse-driven programmable Josephson voltage standard *Appl. Phys. Lett.* **68** 3171–3
- [24] Storm L 1986 Precision measurements of the Boltzmann constant *Metrologia* **22** 229–34
- [25] Middleton D 1996 *An Introduction to Statistical Communication Theory* (Piscataway, NJ: IEEE)